Structure and magnetism of small rhodium clusters

F. Aguilera-Granja,[1] J. L. Rodríguez-López,[2] K. Michaelian,[3] E. O. Berlanga-Ramírez,[1] and A. Vega[4]
[1]*Instituto de Física, Universidad Autónoma de San Luis Potosí, 78000 San Luis Potosí, Mexico*
[2]*Texas Materials Institute, The University of Texas at Austin, 78712-1063 Austin, Texas*
[3]*Instituto de Física, Universidad Nacional Autónoma de México, 20-364, 01000 D.F., Mexico*
[4]*Departamento de Física Teórica, Atómica, Molecular y Nuclear, Universidad de Valladolid, E-47011 Valladolid, Spain*
(Received 1 November 2000; revised manuscript received 10 July 2001; published 17 December 2002)

We report a systematic study of the structural and magnetic properties of free-standing rhodium clusters (Rh_N, $4 \leqslant N \leqslant 26$). The geometrical structures of the global minima and lowest energy isomers were obtained with a semiempirical Gupta potential and employing a global evolutive search algorithm. The spin-polarized electronic structure and related magnetic properties of these geometries were calculated by solving self-consistently a spd tight-binding Hamiltonian. We determined the possible coexistence of different isomers and found that inclusion does not, in general, change significantly the magnetic moments obtained for the global minima structures. Results are compared with the experiment and with other theoretical calculations available in the literature.

DOI: 10.1103/PhysRevB.66.224410 PACS number(s): 75.50.−y, 36.40.Cg

I. INTRODUCTION

The tailoring of new magnetic materials with novel properties is one of the cornerstones of materials science. The Stoner criterion for the existence of spontaneous ferromagnetism is only fulfilled in a few of the $3d$ bulk transition metals (TM)—Fe, Co, and Ni.[1,2] None of the $4d$ and $5d$ solids are magnetic spontaneously.[2] However, since the 1980's, the experimental growth and characterization of low-dimensional systems (surfaces, films, and small clusters)[3–14] with reduced coordination and symmetry, and relaxed interatomic distances, opens the possibility of stabilizing magnetic phases in certain *a priori* nonmagnetic $4d$ and $5d$ transition metals systems.[5] Examples of experimental evidence for the $4d$ ferro-magnetism in two-dimensional Ru and Rh structures supported on substrates can be found in Refs. 12–14.

The study of magnetism in clusters is a two step problem: (i) the identification of the lowest energy geometrical structures and (ii) the determination of the respective electronic properties. These steps are not independent, although it is a common approximation to separate them due to the computational costs involved in fully self-consistent calculations, even in the case of very small clusters.[15–18] The *ab initio* methods are limited to very small cluster sizes[19] so that for the cluster sizes in the range involved in experiment, there is little alternative but to perform semiempirical calculations.[15,16]

In the particular case of $4d$ magnetism, rhodium has been the most studied, and at the same time, the most controversial of this series. Many investigations in Rh clusters were motivated by the pioneering theoretical works by Galicia,[20] Reddy *et al.*,[21] and the experimental results by Cox and co-workers.[5] However, most of the electronic calculations for Rh clusters available in the literature have been performed assuming fixed geometries,[22–24] or optimizing just the bond lengths.[25–32] Recently, Reddy *et al.*[33] have combined the techniques of molecular-dynamics (MD) for the geometrical part and density-functional theory (DFT) for the electronic part. With this approach, they could study small Rh clusters only up to 13 atoms.

The available theoretical studies of free-standing rhodium clusters, most of these performed within the DFT-LDA approximation, demonstrate a wide dispersion in the magnetic properties.[20,22,25,26,28,31] This suggests a strong sensitivity of the calculated magnetic properties of Rh to the approximations of the method and to the presumed underlying geometric structure. The geometrical structure of free-standing clusters is an elusive property since experimental information is indirect and not sufficient to determine the structure precisely. In another context, *ab initio* calculations for the Rh dimer supported on Ag(001) have also shown that this metal does not always follow the general trends of magnetism with respect to the coordination number and interatomic distances.[34] The local magnetic moment in the supported dimer decreases while increasing the interatomic distance, in contrast to the general behavior of the $3d$ elements. Therefore, we believe that a systematic study of both the geometrical structure and magnetic properties is required for free-standing Rh_N clusters in a size range similar to that studied experimentally. This is the objective of the present work.

We have performed a systematic search for the global minimum and the three lowest energy isomers of Rh_N clusters in the range of $4 \leqslant N \leqslant 26$ atoms. The geometries have been obtained using a global search method on the energy surface of a many-body Gupta potential.[35] The spin-polarized electronic properties were then calculated for these geometries using a Hubbard type Hamiltonian for the $4d$,$5s$, and $5p$ valence electrons within the unrestricted Hartree-Fock approximation. The magnetic moments of the different isomers were weighted according to their relative normalized populations (RP's) calculated using the free energies and assuming an equilibrium distribution at room temperature. This allowed comparison of the magnetic moments obtained for the global minimum geometries with that obtained by including the coexistence of the lowest energy isomers. The magnetic behavior of the Rh_{13} cluster as a function of interatomic distance is investigated. In the next section we briefly de-

scribe the methods and approximations used. The results obtained for the geometrical structures and the magnetic properties are presented and discussed in Sec. III. In Sec. IV we summarize the main conclusions of this work.

II. GEOMETRIC AND ELECTRONIC STRUCTURE CALCULATIONS

A. Geometrical structure

The global minimum geometrical structures of the clusters have been obtained by making 80 000 global optimizations starting from distinct random initial configurations of the atoms within a sphere large enough to include all conceivable low energy geometries. The optimizations were done with an evolutive, symbiotic algorithm,[36] an efficient variant of the genetic algorithm,[37] that takes advantage of the tight coupling of nearest neighbor atoms through the short range of the interaction. The algorithm employs a hybrid approach consisting of the global genetic algorithm with stochastic moves on the potential energy surface which avoid entrapment in high-energy local minima, combined with local conjugate gradient relaxation once the global part has reached the attraction basins of the lowest-energy minima. Details of the application of the symbiotic algorithm to the optimization of metal clusters using the Gupta potential are given in Ref. 38.

The attractive, many-body part of the Gupta potential is formulated in the second moment approximation of the density of electronic states within the tight-binding scheme, while a Born-Mayer term describes the repulsive pair interactions. This potential is expressed as

$$V=\sum_{i=1}^{n}\left[A\sum_{j(\neq i)=1}^{n}\exp\left[-p\left(\frac{r_{ij}}{r_{0n}}-1\right)\right]-\left(\xi^2\sum_{j(\neq i)=1}^{n}\exp\left[-2q\left(\frac{r_{ij}}{r_{0n}}-1\right)\right]\right)^{1/2}\right]. \quad (1)$$

The parameters $p=18.45$, $q=1.867$, $\xi=1.66$ eV, and $A=0.0629$ eV for rhodium are obtained by fitting to the bulk cohesive energy, lattice parameters, and elastic constants.[35] The radii are expressed in reduced units where $r_{0n}=1$.

The use of a potential to model the structure of the Rh nanoclusters was necessary in this work since *ab initio* and truly global optimizations can only be performed on very small clusters ($\leqslant 8$ atoms) with existing computational resources. The Gupta potential is considered to be semiempirical since it is based on the second moment of the electron density of states in the tight-binding scheme, while its parameters are fit to empirical data. The tight-binding scheme takes into account the electronic structure of the system and the quantum-mechanical nature of the bonding. In addition to this physical reason, our choice of the Gupta potential was based on our very successful application of this potential, combined with the parametrizations of Cleri and Rosato,[35] to various metals from the periodic table: Au, Ag, and Ni;[38] Zn and Cd;[39] Na;[40] Pt and Pd[41]). Results for the geometries of Rh nanoclusters obtained with other many-body potentials (for example, the Sutton-Chen potential), at least at the small sizes presented in this paper, are in basic agreement with those of our calculations (see below and Ref. 42). Further, we have shown[43] that most metals of the periodic table follow the icosaheral growth pattern, which we found for Rh, at sizes greater than about 10 atoms (see below). The only exceptions (up to 98 atoms) are encountered at $N=38$ and around $N=75$ for which the truncated octahedron and Marks decahedral structures, respectively, are of lower energy. For $N=38$ atoms, although not reported in this work, our results predicting the truncated octahedral geometry are in agreement with other, more complex Gupta parametrizations by Chien *et al.*[44] For $N=24$ and 26, our global minima and first isomers results are inverted with respect to those reported by Chien *et al.* The only metals we have found which do not follow this trend are Au, Cd, and Zn. These metals appear to have disordered global minimum structures for all sizes, at least up to 100 atoms.[38,39]

For the metals Au, Cd, Zn, Na, Pt, and Pd, we have checked the results of the Gupta potential, incorporating the parametrizations of Cleri and Rosato,[35] with density functional calculations carried out at both the LDA and the GGA levels.[39,41,45] The validation of the potential from this perspective is based on three findings. First, all low-energy minima we have found for the Gupta potential are also minima with density functional theory (both at the LDA and GGA levels). Second, the order in energy of the three lowest energy isomers is basically the same except for a few exceptional cases in which two isomers are almost degenerate in energy.[45] Finally, we have plotted the distances from the center of mass of all of the atoms of Au_{101} obtained with the Gupta potential, and the same obtained with density functional theory at the GGA level.[46] The almost exact correspondences are very convincing in validating the Gupta potential for these metals. This result gives us confidence that the Gupta potential also models Rh well.

From still another perspective, we have compared the calculated structure factors for the global minima of Au_{38} and Au_{75} obtained with the Gupta potential with those obtained from x-ray diffraction experiments. The results of the Gupta potential show very good agreement with experiment.[38]

The reliability of the algorithm in locating the global minimum of metal nanoclusters of sizes up to 75 atoms has been reviewed in Ref. 38 and can be considered as being good, because the lowest-energy minima are found many times.

B. Electronic structure

The spin-polarized electronic structure of Rh clusters was determined by solving self-consistently a tight-binding Hamiltonian for the $4d$, $5s$, and $5p$ valence electrons in a mean-field approximation. In the usual second quantization notation, this Hamiltonian can be expressed as follows:

$$H=\sum_{i\alpha\sigma}\varepsilon_{i\alpha\sigma}\hat{n}_{i\alpha\sigma}+\sum_{\substack{\alpha\beta\sigma\\ i\neq j}}t_{ij}^{\alpha\beta}\hat{c}_{i\alpha\sigma}^{\dagger}\hat{c}_{j\beta\sigma}, \quad (2)$$

where $\hat{c}_{i\alpha\sigma}^{\dagger}$ is the operator for the creation of an electron with spin σ and orbital state α at the atomic site i, $\hat{c}_{j\beta\sigma}$ is the

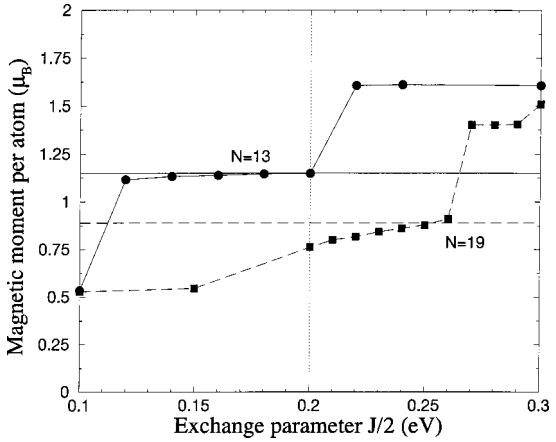

FIG. 1. Magnetic moment per atom as a function of the exchange parameter J_{dd} for the icosahedral ($N=13$) and double-icosahedral ($N=19$) clusters. We used the nearest neighbor distances reported by Jinlong (Ref. 25). The horizontal lines correspond to the solutions of Jinlong (Ref. 25) for $N=13$ (solid line) and $N=19$ atoms (dashed line), respectively. The vertical line is our best simultaneous fit to both values of the magnetic moment.

annihilation operator, and $\hat{n}_{i\alpha\sigma}$ is the number operator. The hopping integrals $t_{ij}^{\alpha\beta}$ between orbitals α and β at sites i and j describe the electronic delocalization within the system, which is relevant for itinerant magnetism. In this work, we considered hopping integrals up to third nearest-neighbor distances. These integrals are assumed to be spin independent and have been fitted to reproduce the band structure of bulk Rh.[47] However, since interatomic distances in the clusters differ slightly from the bulk, the variation of hopping integrals with the interatomic distance r_{ij} has been explicitly considered using the typical power law $(r_0/r_{ij})^{l+l'+1}$, where r_0 is the bulk equilibrium distance and l, l' are the orbital angular momenta of the $(i\alpha\sigma)$ and $(j\beta\sigma)$ states involved in the hopping process. The spin-dependent diagonal terms account for the electron-electron interaction through a correction shift of the energy levels

$$\varepsilon_{i\alpha\sigma}=\varepsilon_{i\alpha}^{0}+z_{\sigma}\sum_{\beta}\frac{J_{\alpha\beta}}{2}\mu_{i\beta}+\Omega_{i\alpha}. \tag{3}$$

Here, $\varepsilon_{i\alpha}^{0}$ are the bare orbital energies of paramagnetic bulk Rh. The second term is the correction shift due to the spin polarization of the electrons at site i ($\mu_{i\beta}=\langle n_{i\beta\uparrow}\rangle - \langle n_{i\beta\downarrow}\rangle$). $J_{\alpha\beta}$ are the exchange integrals and z_{σ} is the sign function ($z_{\uparrow}=1$, $z_{\downarrow}=-1$). As usual, the exchange integrals involving s and p electrons were neglected taking into account only the integral corresponding to d electrons (J_{dd}). Note that although the sp exchange integrals are neglected, spin polarization of the delocalized sp states will exist as a consequence of hybridization with the d states. Usually J_{dd} is obtained by fitting to the bulk magnetic moment. However, since rhodium bulk metal is paramagnetic, we have taken $J_{dd}=0.40$ eV so that it gives simultaneously the best fit to the magnetic moments of the Rh_{13} and Rh_{19} clusters as calculated by Jinlong *et al.*[25] through the DFT-LSDA method (see Fig. 1). For Rh_{13} we have the same value as Jinlong whereas for Rh_{19} we slightly understimate the magnetic moment, this value of J_{dd} corresponds to the best simultaneous fitting considering the dependence shown in the Fig. 1. Those cluster sizes have been selected because the icosahedral and double icosahedral geometries are typical in almost all calculations. Finally, the site- and orbital-dependent self-consistent potential $\Omega_{i\alpha}$ assures the local electronic occupation, fixed in our model by interpolating between the isolated atom and the bulk according to the actual local number of neighbors at site i.

The spin-dependent local electronic occupations are self-consistently determined from the local densities of states

$$\langle\hat{n}_{i\alpha\sigma}\rangle=\int_{-\infty}^{\varepsilon_F}\mathcal{D}_{i\alpha\sigma}(\varepsilon)d\varepsilon, \tag{4}$$

which are calculated at each iteration by using the recursion method.[48] In this way, the distribution of the local magnetic moments ($\mu_i=\Sigma_{\alpha}\mu_{i\alpha}$) and the average magnetic moment per atom ($\bar{\mu}=1/N\Sigma_i\mu_i$) of the Rh_N clusters are obtained at the end of the self-consistent cycle.

The description of the magnetic properties of low-dimensional $4d$ transition metal systems requires the same ingredients as for the $3d$ series, in particular, the explicit consideration of the electronic delocalization in order to account for the itinerant character of the magnetism of these materials and also the symmetry of each system which plays an important role due to the directional bonding. The fact that this tight-binding model has been successfully applied to the study of $3d$ TM clusters in both the free-standing configuration[15] and supported on a substrate[18] give us confidence in its utilization for the investigations presented here.

III. RESULTS AND DISCUSSION

There are no experimental works concerning the geometrical structures of Rh_N clusters. The reactions of ammonia and water molecules on hydrogen saturated clusters and photo-ionization experiments are used to obtain clues to the geometrical structures of Fe, Co, and Ni clusters.[49,50] These works give evidence of polyicosahedral structure in ammoniated and bare Ni and Co clusters.

On the theoretical side, recently the Gupta potential has been used for Ni_N clusters and for noble metal clusters like Au_N and Ag_N by Michaelian and co-workers[38] using the symbiotic algorithm applied in the present work. In the case of Au_N clusters, they have found evidence of disordered global minima for $N=19$, 38, and 55 atoms.[38,45] Polyicosahedral atomic growth is revealed for Ni and Ag clusters, at least for the global minima and up to sizes of $N=55$ atoms. Such an icosahedral growth pattern is also obtained here for the global minima structures for Rh_N up to $N=26$ atoms (see structures denoted as [1] in Fig. 2). In general, this pattern is followed by incorporating atoms (one by one) to a stable closed shell structure, reaching in this way the main and intermediate icosahedral sizes, i.e., Rh_{13}, Rh_{19}, Rh_{23}, and Rh_{26}. For the second isomers (denoted as [2] in Fig. 2) there is not a well defined sequence of structures, although isomers with $N=7$, 11, 15, and 16 seem to follow a growth pattern

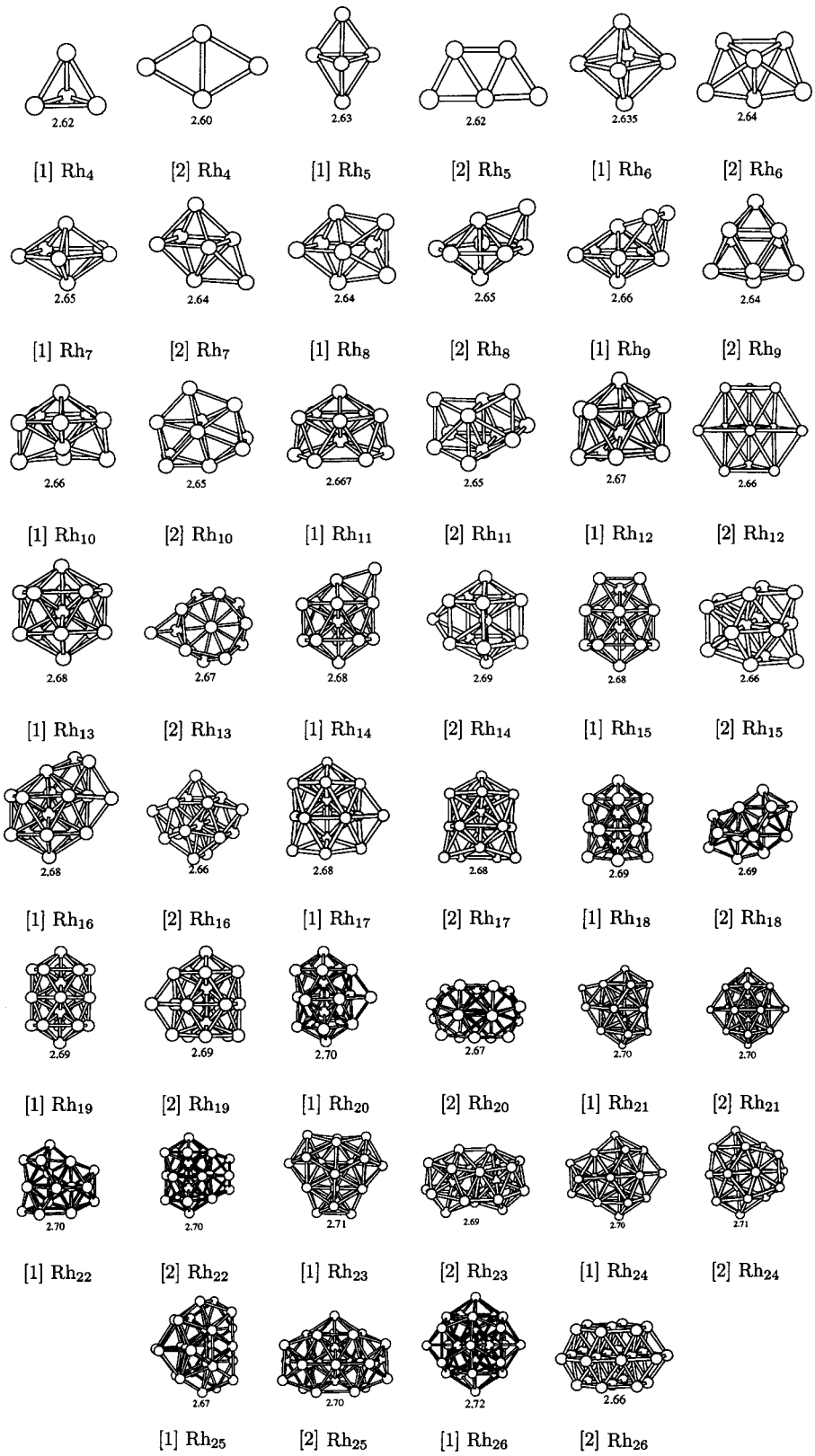

FIG. 2. Optimized geometrical structures for Rh_N clusters ($4 \leqslant N \leqslant 26$ atoms). The global minima are denoted as [1] and the second isomers as [2]. The number below the structure is the average bond distance in Å.

with a square pyramid (C_{4v}) as a base unit. In general there are threefold, fourfold, and fivefold local symmetries in this isomeric sequence; also distorted icosahedrals are present, particularly at large sizes, except for Rh_{26} which has an hcp symmetry. For the third and fourth isomeric sequences (not shown in the figure) there is no well defined family of structures.

In Fig. 3 we plot two of the most representative geometrical properties for the free-standing clusters shown in Fig. 2; the average atomic coordination and the average nearest-

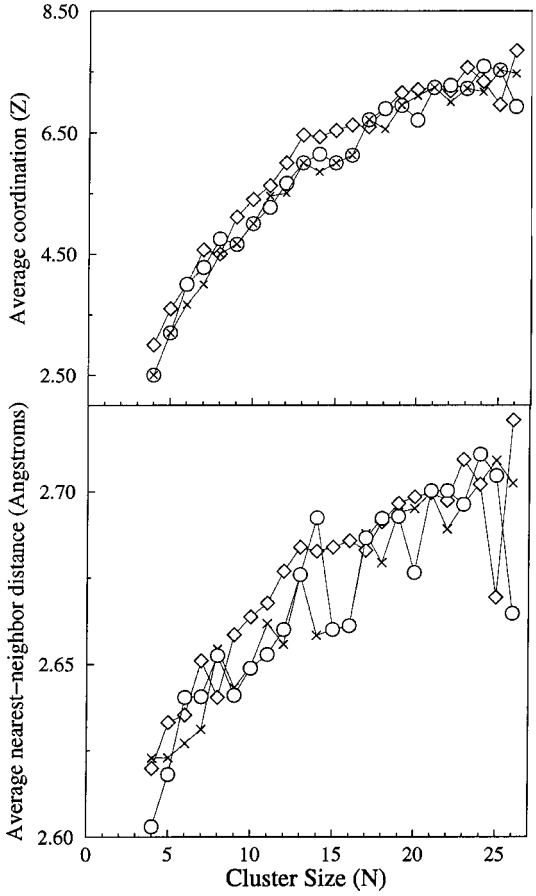

FIG. 3. Structural properties for the three lowest-energy isomers of Rh_N clusters. The upper panel shows the average atomic coordination and the average nearest-neighbor distance is shown in the lower panel. The rhombus symbols correspond to the global minimum geometries, the empty circles to the second isomer and the cross to the third isomer. The bond distance of the fcc Rh bulk is $r_0 = 2.69$ Å.

neighbor distance. Notice that the average coordination in the three different series of isomers is generally the same regardless of the different geometries. For the nearest-neighbor distances, small variations from the bulk are observed although the convergence to the bulk value is already reached at small sizes, around Rh_{13}.

For $N \leqslant 7$ our global minima are the same as those reported by Reddy *et al.*[33] (except at $N=5$), who used the Gupta potential form proposed by Llois and Weissman[51] in a MD search combined with bond optimization using DFT.[33] The Gupta potential they used has a (2/3) exponent in the many-body band term, instead of the usual (1/2)—see Eq. (1). The only structure that changes after DFT relaxation is the hexahedron Rh_5 (D_{3h}), which stabilizes in a square pyramid structure (C_{4v}), whereas our calculation predicted a hexahedron as the global minimum and a planar triple triangular structure as the second isomer. For $9 \leqslant N \leqslant 13$ our clusters are decahedral (pentagonal bipyramid) plus additional adjacent atoms around the main symmetry axis until an icosahedral is reached. In this size range, all our geometries agree with those obtained by Reddy *et al.*[33] and those by Doye and Wales[42] using a Monte Carlo approach and the Sutton-Chen potential. Although our geometries and those of Reddy *et al.* are similar (the only difference is at $N=5$), the cluster size is different. Our clusters are systematically larger than those of Reddy *et al.*[33] Our average bond length goes from 2.62 Å- in the tetrahedral to 2.69 Å- in the icosahedral, whereas Reddy *et al.*'s bond length goes from 2.5 to 2.68 Å for the same size range. We believe that these discrepancies come from the different versions of the Gupta potential used, due to the energy band term. This term incorporates a many-body summation, which is proportional to the hopping integrals through the second moment of the density of states, and the exponent (2/3)—or (1/2) in our case—affects indirectly the bond distances.[35,51]

Results for $14 \leqslant N \leqslant 19$ show an icosahedral growth pattern for the lowest-energy structure until a double icosahedron is reached at $N=19$, with an average nearest-neighbor distance similar to that of the bulk. For $N=23$ and $N=26$ atoms we find a polyicosahedral structure formed by three and six interpenetrated double-icosahedral sections, respectively. The only theoretical study of the geometrical structure of free-standing Rh_N clusters with sizes larger than $N=13$ atoms is that of Ref. 42 using Monte Carlo minimization and the family of Sutton-Chen potentials for clusters with $N \leqslant 80$ atoms. The agreement with these results is good, the only differences are at $N=23$ and $N=26$ atoms. For $N=26$ our second isomer corresponds to the global minimum obtained by Doye and Wales, a hexagonal closed packed structure.

Table I summarizes the results we obtained for our global minima compared with other published calculations. In the case of Rh_4, there is general agreement that the lowest-energy structure is a tetrahedron (T_d) using both *ab initio* and semiempirical methods with small dispersion in the calculated binding energies per atom. This structure is nonmagnetic (see Table I). Some of these calculations have led to magnetically open structures such as D_{4h} (square) (Refs. 25,29,31,33) and D_{2h} (rhombus) (Refs. 25,29) as our result for the second isomer (see Fig. 2 for [2] Rh_4 and discussion below). These magnetically open structures are energetically close to the global minimum, although not close enough to allow transitions through thermal excitations from one structure to another at room temperature. However, this kind of structural transition may be possible under strain forces (e.g., supported clusters) or pressure conditions (e.g., inside a matrix). This has been studied by Wildberger *et al.*[52] for Rh ad-atoms on Ag(001) with the KKR-Green's function method. Interestingly, they have found that compact structures such as the square have significant magnetic moment.

For Rh_5, all the calculations predict a magnetic moment. We obtain a triangular bipyramid (hexahedron) as the global minimum, as found by Jinlong *et al.*[25] through the LSDA approximation, with the same magnetic moment although with different cluster size. Both Refs. 31 and 33 have obtained a square pyramid C_{4v} as the most stable structure, with similar equilibrium bond length and magnetic moment. For Rh_6 we find a geometry that is widely obtained as the lowest-energy structure by different methods and approximations,[25,26,28,31] although with different cluster size. Our magnetic moment is in agreement with the results ob-

TABLE I. Symmetry, average bond distance d_n (Å), binding energy E_b (eV/atom), and magnetic moments $\overline{\mu}$ (μ_B/atom) for the global minima structures from $N=4$ to 26 atoms, compared with other results. The method of calculation used by Galicia (Ref. 20) is SCF-$X\alpha$-SW, by Lee (Ref. 22) LCGO-DFT, by Jinlong *et al.* (Ref. 25) and Li (Ref. 26) DV-LSDA, by Reddy (Ref. 21) and Zhang (Ref. 28) LCAO-MO-DFT, by Nayak (Ref. 29), Chien (Ref. 31), and Reddy *et al.* (Ref. 33), GGA-DFT. Finally Piveteau (Ref. 27), Villaseñor *et al.* (Ref. 30), and Guirado-López *et al.* (Ref. 32) have used the TB-HFA method. Experimental results are as given in Ref. 5.

N	Symmetry	d_n	E_b	$\overline{\mu}$	Reference
4	T_d	2.48	2.95	0.00	25
	T_d	2.49	2.41	0.00	29
	T_d	2.50	2.42	0.00	31
	T_d	2.50	2.91	0.00	33
	T_d	2.62	2.71	0.06	Present work
5	D_{3h}	2.52	3.06	0.60	25
	C_{4v}	2.54	2.70	1.00	31
	C_{4v}	2.55	3.13	1.40	33
	D_{3h}	2.63	2.95	0.22	Present work
6	O_h	2.54	3.45	0.00	25
	O_h	2.63	3.32	0.00	26
	O_h	2.60	4.03	0.99	28
	O_h	2.60	2.88	1.00	31
	D_{4h}	2.58	3.28	0.00	33
	O_h	2.63	3.17	1.48	Present work
7	D_{5h}	2.58	3.43	1.28	25
	D_{5h}	2.61	3.33	1.28	33
	D_{5h}	2.65	3.31	0.05	Present work
8	T_d	2.58	3.46	1.25	25
	D_{2d}	2.61	3.40	0.75	33
	D_{2d}	2.64	3.39	0.89	Present work
9	O_h	2.64	3.33	0.56	26
	D_{4d}	2.55	2.38	0.66	30
	C_{2v}	2.63	3.40	1.00	33
	C_{2v}	2.66	3.50	1.62	Present work
				0.80 ± 0.20	Experiment
10	D_{4d}	2.58	3.77	0.60	25
	C_{3v}	2.63	3.50	0.20	33
	C_{3v}	2.66	3.59	0.41	Present work
				0.80 ± 0.20	Experiment
11	C_{2v}	2.64	2.43	0.73	30
	C_{2v}	2.63	3.55	0.29	33
	C_{2v}	2.66	3.66	1.53	Present work
				0.80 ± 0.20	Experiment
12	C_{5v}	2.56	3.86	0.67	25
	C_{5v}	2.65	3.58	0.63	33
	C_{5v}	2.67	3.76	0.24	Present work
				0.59 ± 0.12	Experiment
13	O_h	2.69 [a]		1.00	20
	I_h	2.66	3.27	1.61	21
	I_h	2.66	4.01	1.15	25
	I_h	2.66	3.45	0.43	26
	I_h	2.64	2.17	1.69	27
	bcc	2.50	2.41	0.62	30
	O_h	2.69 [a]		0.69	22
	O_h	2.66		0.77	32
	I_h	2.69	3.65	1.15	33
	I_h	2.68	3.89	1.26	Present work
				0.48 ± 0.13	Experiment
14	C_{3v}	2.68	3.88	0.39	Present work
				0.50 ± 0.12	Experiment
15	O_h	2.58	2.44	0.80	30
	C_{3v}	2.68	3.92	0.31	Present work
				0.71 ± 0.09	Experiment
16	C_s	2.68	3.95	0.39	Present work
				0.64 ± 0.10	Experiment
18		2.69	4.01	0.31	Present work
				0.35 ± 0.12	Experiment
19	D_{5h}	2.69 [a]	4.45	0.89	25
	O_h	2.65	3.85	0.43	26
	O_h	2.61	2.52	0.95	30
	O_h			1.17	32
	D_{5h}	2.69	4.08	0.61	Present work
				0.61 ± 0.08	Experiment
20		2.7	4.09	0.08	Present work
				0.16 ± 0.16	Experiment
22		2.69	4.13	0.02	Present work
				0.27 ± 0.14	Experiment
23	bcc	2.50	2.52	0.35	30
	D_{3h}	2.71	4.17	0.03	Present work
				0.13 ± 0.13	Experiment
26	D_{6d}	2.72	4.22	0.03	Present work
				0.25 ± 0.12	Experiment

[a]Nonoptimized bond, bulk distance used.

tained by Zhang *et al.*[28] and Chien *et al.*[31] Rh_{13} is one of the most studied clusters because it is considered as the seed for different cluster growth patterns, i.e., O_h^{fcc}, I_h^{ico}, D_{3h}^{hcp}, and even O_h^{bcc} (Ref. 30) symmetries. A wide dispersion in the calculated magnetic moments is present in the literature. In almost all works, differences in the interatomic distance are small ($\approx 2\%$) compared to that of the bulk. We found good agreement with results presented in Refs. 33 and 53 concerning the magnetic moment and cluster symmetry I_h. The relationship between bond length relaxations, symmetry and magnetism has been studied for this size in the case of $3d$ (Refs. 19,54) and $4d$ (Ref. 53) systems. This point will be discussed in more detail below. Finally, $N=19$ atoms is another extensively studied geometry in TM clusters because the icosahedral growth pattern give rise to a double icosahedron. Again, the agreement in size, binding energy and magnetic moment with *ab initio* results from Jinlong *et al.* is remarkable, although this time they used a constrained structure. Other works using a fcc geometry differ significantly from experiment. Our result compares well with the experimental behavior, both in magnitude, and as being a maxi-

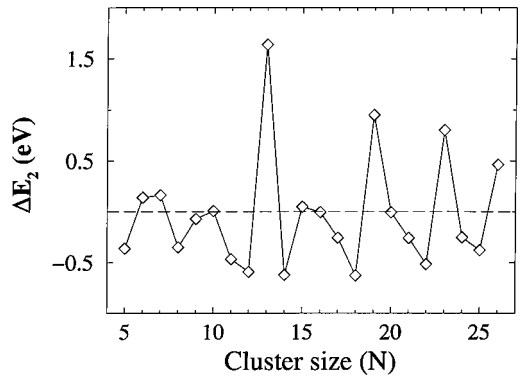

FIG. 4. Relative stability of the global minima Rh_N clusters with respect to their neighbors. ΔE_2 is defined as $\Delta E_2 = E(N+1) + E(N-1) - 2E(N)$. Peaks correlate to main and intermediate sizes at $N = 13$, 19, 23, and 26 atoms.

mum at this size. The magnetic behavior obtained from Rh_{15} to Rh_{26} follows the experimental trend qualitatively well as a function of cluster size, describing the experimentally observed minima and maxima.

In Fig. 4 we have plotted the relative stability of each global minimum Rh_N cluster with respect to its adjacent clusters Rh_{N-1} and Rh_{N+1}. Maxima correlate to the main and intermediate icosahedral sizes ($N = 13$, 19, 23, and 26 atoms), structures which have been recognized as having high stability in previous theoretical works.[42]

The usual experimental technique for cluster generation, laser vaporization in a flow system, involves many control variables (gas transport pressure, cluster concentration, internal and source temperatures, etc.). Therefore, cluster growth is a very complex process where coexistence of different isomers is possible, as has been shown in structural[50] and magnetic[5] experimental works with Ni and Co clusters. Although the growth process is far from equilibrium, once formed, the clusters are in a thermal bath which allows them to evolve to an equilibrium distribution of the isomers, before the measurement of the magnetic moment is obtained. In this context, the relative populations of the four lowest-energy isomers of each size have been calculated assuming an equilibrium distribution at 300 K. Room temperature seems to be a reasonable value for the internal cluster temperature as has been discussed by several authors.[5,55] The free energy F was calculated according to[56]

$$F = V + \sum_i \frac{\hbar\omega_i}{2} + k_B T \sum_i \ln\left[1 - \exp\left(\frac{-\hbar\omega_i}{k_B T}\right)\right], \quad (5)$$

where the first term represents the potential energy, the second term is the zero point energy, and the third, the vibrational contribution to the entropy. The frequencies of the normal modes ω_i were obtained in the harmonic approximation from the eigenvalues of the Hessian evaluated at the minima in the potential energy surface. In Table II the relative isomer populations up to the fourth isomer are tabulated. It is note worthy that there is not an appreciable coexistence of isomers over most of the size range studied here, the only exceptions being at the sizes of $N = 17$, 18, 21, 24, and 25 atoms. This is due to the influence of the enthropic contribution of the low-frequency normal modes of the isomers to the free energy at these sizes where the potential energies of the global minimum and next isomer are almost degenerate. We did not find a significant contribution of the fourth isomer to the populations, the exceptional case being at $N = 17$ atoms with $\approx 2.7\%$. Thus, the fourth and higher-energy isomers were not considered. Our results indicate that at most sizes, there should be few isomers other than the global minimum at the temperature of experiment.

TABLE II. Magnetic moment per atom $\overline{\mu}$ (μ_B) and their respective relative normalized coexistence population RP at room temperature for the global minimum structures (second and third columns) and for the second isomer (fourth and fifth columns). For the third and fourth isomers (sixth and seventh columns) we present just the normalized coexistence population. Note that there are significant contributions of the third isomer just in $N = 17$, $N = 21$, and $N = 25$ atoms. The magnetic moment per atom for the third isomers that have contributions different than zero are $\overline{\mu}_{17}^{[3]} = 0.83\ \mu_B$, $\overline{\mu}_{21}^{[3]} = 0.02\ \mu_B$, and $\overline{\mu}_{25}^{[3]} = 0.45\ \mu_B$, respectively. Within the present scheme, fourth isomer does not contribute with isomerization.

N	$\overline{\mu}^{[1]}$	$RP^{[1]}$	$\overline{\mu}^{[2]}$	$RP^{[2]}$	$RP^{[3]}$	$RP^{[4]}$
4	0.00	1.0	0.5	0.0	0.0	0.0
5	0.59	1.0	0.57	0.0	0.0	0.0
6	0.99	1.0	0.33	0.0	0.0	0.0
7	1.04	1.0	0.43	0.0	0.0	0.0
8	1.15	0.99	0.46	0.01	0.0	0.0
9	0.30	1.0	0.76	0.0	0.0	0.0
10	0.57	1.0	0.13	0.0	0.0	0.0
11	0.48	1.0	0.61	0.0	0.0	0.0
12	1.04	1.0	0.66	0.0	0.0	0.0
13	1.15	1.0	1.00	0.0	0.0	0.0
14	1.14	1.0	0.86	0.0	0.0	0.0
15	0.92	1.0	0.73	0.0	0.0	0.0
16	0.69	1.0	0.48	0.0	0.0	0.0
17	0.45	0.75	0.59	0.14	0.07	0.03
18	0.68	0.86	0.23	0.14	0.0	0.0
19	0.76	1.0	0.59	0.0	0.0	0.0
20	0.74	1.0	0.56	0.0	0.0	0.0
21	0.40	0.8	0.56	0.10	0.1	0.0
22	0.51	0.93	0.35	0.07	0.0	0.0
23	0.25	1.0	0.80	0.0	0.0	0.0
24	0.08	0.64	0.04	0.36	0.0	0.0
25	0.42	0.0	0.41	0.33	0.66	0.01
26	0.34	1.0	0.08	0.0	0.0	0.0

Magnetism in low-dimensional systems is influenced by a number of factors such as the symmetry, local coordination, and interatomic distances. For $3d$ systems there are two widely accepted semiempirical rules that correlate the magnetic moment with the structure: decreasing coordination and increasing interatomic distance enhances the magnetic moments because both factors tend to reduce electron delocalization. Our results indicate that these rules do not seem to hold in general for Rh_N clusters. This has also been noticed

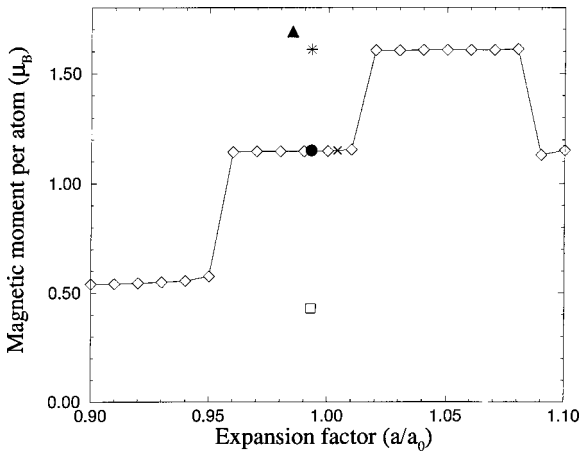

FIG. 5. Behavior of the $\overline{\mu}$ for the Rh_{13} icosahedron cluster as a function of the interatomic distance ($\diamond$). Expansion factor equals one corresponds to our solution at the present work. For comparison, we include solutions by Reddy *et al.* (Ref. 21) (*), Jinlong *et al.* (Ref. 25) (●), Li *et al.* (Ref. 26) (□), Piveteau *et al.* (Ref. 27) (▲), and Jena *et al.* (Ref. 33) (×).

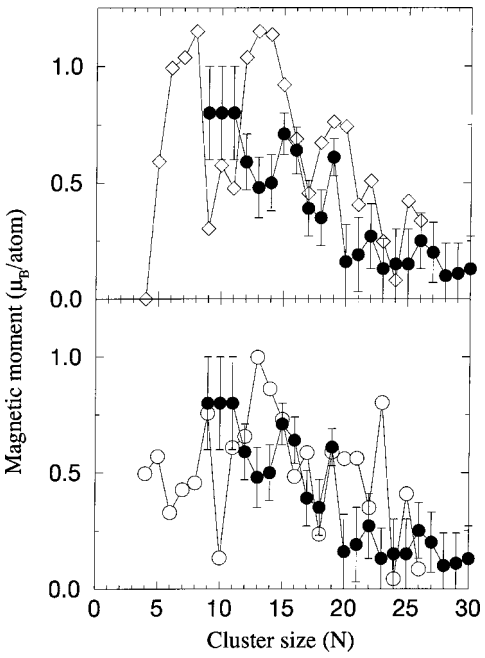

FIG. 6. The average magnetic moment per atom for the global minimum (upper panel) structures of Rh_N clusters ($\diamond$) compared with the experiment (Ref. 5) (●). In the lower panel, the same is shown for the corresponding second isomers (○).

by Stepanyuk *et al.*[34] for Rh nanoclusters supported on Ag(001). In contrast to 3*d* clusters such as Ni, where we have obtained in a previous work a linear decreasing dependence of $\overline{\mu}$ with Z (see Ref. 15), here we obtain a large dispersion of the results, accompanied sometimes with oscillations.

As we have already pointed out, there is a wide dispersion in the available theoretical results for the magnetic moment. We now further analyze this aspect with respect to the case of Rh_{13} for which the icosahedral structure is obtained in most of the theoretical approaches. The structural symmetry of the cluster is thus excluded as the possible source of the discrepancy among the different theoretical calculations. Different calculations, however, give slightly different interatomic distances for icosahedral Rh_{13}. In order to test how sensitive the magnetic properties are to changes in the interatomic distance and if these slight changes may be the origin of the discrepancies, we have performed uniform compressions and expansions of up to 10% of the global minimum icosahedral structure. Figure 5 shows the resulting magnetic behavior. An expansion factor of 1 corresponds to the global minimum. We have also included the results available in the literature for this cluster at the corresponding interatomic distances. Our results indicate that the differences in the magnetic moments obtained with the different methods are not associated with the different interatomic distances since, over a wide range of compression factors (which includes all the interatomic distances reported in previous works), the magnetic moment does not change appreciably. Therefore, we conclude that the magnetic moment is not very sensitive to changes in the interatomic distance around the reported values and thus, the origin of the dispersion of the results is still unclear.

In Fig. 6 we show the results of the average magnetic moment per atom as a function of the cluster size for optimized global minima (upper panel) and for the second isomer (lower panel), compared with the experimental data up to $N=26$ atoms. In both cases, we obtain the general trend of decreasing magnetic moment, in a nonmonotonic fashion, while increasing the cluster size, the moment nearly vanishing as we approach $N\approx 25$, in good agreement with the experimental findings. As for other transition metal clusters, we obtain an oscillatory behavior. For the global minima structures (upper panel of Fig. 6) the maxima are located at $N=8$, 10, 13, 19, 22, and 25 atoms, and the minima at $N=9$, 11, 17, 21, and 24 atoms. For $N<13$ our results do not correlate well with the experiment which display a flat dependence in the magnetic moment from $N=9$ to $N=11$ atoms with the minimum located at $N=13$. It is worth noticing that the first-principles calculations by Jinlong *et al.*[25] and Reddy *et al.*[33] for $N=13$ also lead to a maximum, as in our case. For larger clusters ($N>14$) we have a very good qualitative agreement with the experiment. The experimental observed maxima at $N=19$ and $N=21$ atoms are well described and the experimental minima at $N=18$, 20, and 24 atoms are fairly well described by our results at $N=17$, 21, and 24, atoms respectively. In general, our absolute values slightly overestimate the experimental ones, except at smaller sizes.

Concerning the second isomer (lower panel in the Fig. 6), we have also an oscillatory behavior of the average magnetic moment per atom as a function of the cluster size with very sharp maxima and minima. It is interesting to analyze the cases of $N=13$ and $N=19$. The geometrical structures of the second isomers are icosahedral clusters with one of the atoms misplaced. When this atom is not misplaced and completes the closed shell of the perfect icosahedral structure (global minima structure) the magnetic moment increases (compare both panels of Fig. 6). These type of geometrical

effects in conection with the magnetic behavior have been also observed and theoretically calculated in Ni clusters. However, in the case of Ni clusters, symmetrical structures lead to a lower magnetic moments, in contrast to Rh clusters. This result gives further support to the unique magnetic behavior of low-dimensional rhodium systems.

As discussed previously, our results indicate that at most sizes, there should be few isomers other than the global minimum at the temperature of the experiment. Therefore, the consideration of the different isomers does not change significantly the magnetic trends obtained for the global minima and the comparison with the experimental results. We have checked this point by weighting the magnetic moments by their corresponding calculated populations shown in Table II.

IV. SUMMARY AND CONCLUSIONS

We have determined the geometrical structures of small Rh clusters with a many-body Gupta potential using a global search method. For the global minimum we found that the icosahedral growth pattern dominates for small clusters. For the second isomeric sequence there is no well defined pattern although, in most cases, the clusters are slightly distorted icosahedral structures, particularly for the larger sizes. For the third isomeric sequence, it is not possible to identify a well defined family of structures.

Using a tight-binding Hamiltonian, we calculated the spin polarized electronic structure of the lowest-energy isomers of the clusters. We obtained the general tendency of the magnetic moment to vanish as the cluster size approaches $N \approx 25$ and good qualitative agreement with the experimental findings for $N \geqslant 14$ atoms. However, the results for the magnetic moment as a function of the cluster size show an oscillatory behavior around the experimental data as a function of the size for $N \leqslant 13$ atoms. The wide dispersion in the published theoretical results for the magnetic moments at smaller sizes clearly indicates that more work has to be done in refining the calculations. However, it may be true that experimental conditions are a poor approximation to equilibrium. Contamination with neighboring cluster sizes could also have a significant effect on damping the oscillations found in the calculations.

The empirical rules relating geometrical factors like local coordination and nearest-neighbor distances with the magnetic moment do not hold in general for rhodium clusters. We have investigated the degree of isomer coexistence assuming an equilibrium distribution at room temperature, and studied its effect on the magnetic behavior. We only find an appreciable coexistence of isomers for the sizes of $N=17$, 18, 21, 24, and 25 atoms. Of these sizes, only the sizes of 17 and 21 atoms the magnetic moment of the second isomer (and at $N=25$ for the third isomer) differ significantly from that of the global minimum. We therefore conclude that the discrepancy between the magnetic moments obtained in experiment and our calculations at small sizes cannot be attributed to the effect of the coexistence of isomers and must be found elsewhere.

ACKNOWLEDGMENTS

The authors acknowledge the financial support from CONACyT, México, under Grant Nos. G25851, 25083E and the Milleniun iniciative (CONACyT) W-8001; also to CICYT, Spain, Project No. PB98-0368-C02, and the Junta de Castilla-León, Spain, Grant No. VA073/02. F.A.G. acknowledges the partial support of FONDECYT-Chile through Grant No. 7010511. E.O.B.G. acknowledges financial support from CoPoCyT-SLP. J.L.R.L. is indebted to the IF-UASLP and its personnel for continuous support. We acknowledge computer time on the Cray T3E at the Texas Advanced Computing Center, The University of Texas at Austin. The authors are grateful to J. Dorantes-Davila for useful discussions.

[1] H. Ibach and H. Lüth, *Solid State Physics*, 2nd ed. (Springer-Verlag, Berlin, 1995).
[2] J. F. Janak, Phys. Rev. B **16**, 255 (1977).
[3] D. M. Cox, D. J. Trevor, R. L. Whetten, E. A. Rohlfing, and A. Kaldor, Phys. Rev. B **32**, 7290 (1985).
[4] L. M. Falicov, D. T. Pierce, S. D. Bader, R. Gronsky, K. B. Hathaway, H. J. Hopster, D. N. Lambeth, S. S. P. Parkin, G. Prinz, M. Salamon, I. V. Shuller, and R. H. Victora, J. Mater. Res. **5**, 1299 (1990), and references therein.
[5] A. J. Cox, J. G. Louderback, and L. A. Bloomfield, Phys. Rev. Lett. **71**, 923 (1993); A. J. Cox, J. G. Louderback, S. E. Apsel, and L. A. Bloomfield, Phys. Rev. B **49**, 12 295 (1994).
[6] W. A. de Heer, P. Milani, and A. Châtelain, Phys. Rev. Lett. **65**, 488 (1990).
[7] J. P. Bucher, D. C. Douglass, and L. A. Bloomfield, Phys. Rev. Lett. **66**, 3052 (1991).
[8] D. C. Douglass, A. J. Cox, J. P. Bucher, and L. A. Bloomfield, Phys. Rev. B **47**, 12 874 (1993).
[9] I. M. Billas, J. A. Becker, A. Châtelain, and W. A. de Heer, Phys. Rev. Lett. **71**, 4067 (1993).
[10] I. M. Billas, A. Châtelain, and W. A. de Heer, Science **265**, 1682 (1994).
[11] S. E. Apsel, J. W. Emmert, J. Deng, and L. A. Bloomfield, Phys. Rev. Lett. **76**, 1441 (1996).
[12] R. Pfandzelter, G. Steierl, and C. Rau, Phys. Rev. Lett. **74**, 3467 (1996).
[13] A. Goldoni, A. Baraldi, G. Comelli, S. Lizzit, and G. Paolucci, Phys. Rev. Lett. **82**, 3156 (1999).
[14] M. Kobayashi, T. Kai, N. Takano, and K. Shiiki, J. Phys.: Condens. Matter **7**, 1835 (1995).
[15] F. Aguilera-Granja, S. Bouarab, M. J. López, A. Vega, J. M. Montejano-Carrizales, M. P. Iñiguez, and J. A. Alonso, Phys. Rev. B **57**, 12 469 (1998).
[16] J. L. Rodríguez-López, F. Aguilera-Granja, K. Michaelian, and A. Vega (unpublished).
[17] A. N. Andriotis and M. Menon, Phys. Rev. B **59**, 15 942 (1999).

[18] R. Robles, R. Longo, A. Vega, and L. J. Gallego, Phys. Rev. B **62**, 11 104 (2000).
[19] F. A. Reuse, S. N. Khanna, and S. Bernel, Phys. Rev. B **52**, 11 650 (1995); F. A. Reuse and S. N. Khanna, Chem. Phys. Lett. **234**, 77 (1995).
[20] R. Galicia, Rev. Mex. Fís. **32**, 51 (1985).
[21] B. V. Reddy, S. N. Khanna, and B. I. Dunlap, Phys. Rev. Lett. **70**, 3323 (1993).
[22] K. Lee, Z. Phys. D: At., Mol. Clusters **40**, 164 (1997).
[23] R. Guirado-López, D. Spanjaard, M. C. Desjonquères, and F. Aguilera-Granja, J. Magn. Magn. Mater. **186**, 214 (1998).
[24] J. Guevara, A. M. Llois, F. Aguilera-Granja, and J. M. Montejano-Carrizales, Solid State Commun. **111**, 335 (1999).
[25] Y. Jinlong, F. Toigo, and W. Kelin, Phys. Rev. B **50**, 7915 (1994).
[26] Z. Q. Li, J. Z. Yu, K. Ohno, and Y. Kawazoe, J. Phys.: Condens. Matter **7**, 47 (1995).
[27] B. Piveteau, M. C. Desjonguères, A. M. Olés, and D. Spanjaard, Phys. Rev. B **53**, 9251 (1996).
[28] G. W. Zhang, Y. P. Feng, and C. K. Ong, Phys. Rev. B **54**, 17 208 (1996).
[29] S. K. Nayak, S. E. Weber, P. Jena, K. Wildberger, R. Zeller, P. H. Dederichs, V. S. Stepanyuk, and W. Hergert, Phys. Rev. B **56**, 8849 (1997).
[30] P. Villaseñor-González, J. Dorantes-Dávila, H. Dreyssé, and G. M. Pastor, Phys. Rev. B **55**, 15 084 (1997).
[31] C.-H. Chien, E. Blaisten-Barojas, and M. R. Pederson, Phys. Rev. A **58**, 2196 (1998).
[32] R. Guirado-López, D. Spanjaard, and M. C. Desjonquères, Phys. Rev. B **57**, 6305 (1998).
[33] B. V. Reddy, S. K. Nayak, S. N. Khanna, B. K. Rao, and P. Jena, Phys. Rev. B **59**, 5214 (1999).
[34] V. S. Stepanyuk, W. Hergert, P. Rennert, J. Izquierdo, A. Vega, and L. C. Balbás, Phys. Rev. B **57**, 14 020 (1998).
[35] F. Cleri and V. Rosato, Phys. Rev. B **48**, 22 (1993).
[36] K. Michaelian, Chem. Phys. Lett. **293**, 202 (1998).
[37] K. Michaelian, Am. J. Phys. **66**, 231 (1998).
[38] K. Michaelian, N. Rendón, and I. L. Garzón, Phys. Rev. B **60**, 2000 (1999).
[39] K. Michaelian, M. R. Beltrán, and I. L. Garzón, Phys. Rev. B **65**, 041403(R) (2002).
[40] J. A. Reyes-Nava, I. L. Garzón, M. R. Beltrán, and K. Michaelian, Rev. Mex. Fis. **48**, 450 (2002).
[41] M. R. Beltrán, K. Michaelian, and I. L. Garzón (unpublished).
[42] J. P. K. Doye and D. J. Wales, New J. Chem. **22**, 733 (1998).
[43] K. Michaelian, M. R. Beltrán, and I. L. Garzón (unpublished).
[44] C. H. Chien, E. Blaisten-Barojas, and M. R. Pederson, J. Chem. Phys. **112**, 2301 (2000).
[45] I. L. Garzón, K. Michaelian, M. R. Beltrán, A. Posada-Amarillas, P. Ordejon, E. Artacho, D. Sánchez-Portal, and J. M. Soler, Phys. Rev. Lett. **81**, 1600 (1998).
[46] J. I. Rodríquez-Hernández, Masters thesis, Instituto Politécnico Nacional, Mexico D.F., 2002.
[47] D. A. Papaconstantopoulos, *Handbook of the Band Structure of Elemental Solids* (Plenum, New York, 1996).
[48] R. Haydock, *Solid State Physics*, edited by E. Ehrenreich, F. Seitz, and D. Turnbull (Academic Press, London, 1980), Vol. 35, p. 215.
[49] E. K. Parks, G. C. Nieman, K. P. Kerns, and S. J. Riley, J. Chem. Phys. **107**, 1861 (1997).
[50] E. K. Parks, B. J. Winter, T. D. Klots, and S. J. Riley, J. Chem. Phys. **96**, 8267 (1992); **99**, 5831 (1993); M. Pellarin, B. Baguenard, J. L. Vialle, J. Lerme, M. Broyer, J. Miller, and A. Perez, Chem. Phys. Lett. **217**, 349 (1994).
[51] J. Guevara, A. M. Llois, and M. Weissmann, Phys. Rev. B **52**, 11 509 (1995).
[52] K. Wildberger, V. S. Stepanyuk, P. Lang, R. Zeller, and P. H. Dederichs, Phys. Rev. Lett. **75**, 509 (1995); V. S. Stepanyuk, W. Hergert, P. Rennert, K. Wildberger, R. Zeller, and P. H. Dederichs, Phys. Rev. B **59**, 1681 (1999).
[53] Y. Jinlong, F. Toigo, Wang Kelin, and Zhang Manhong, Phys. Rev. B **50**, 7173 (1994).
[54] B. I. Dunlap, Phys. Rev. A **41**, 5691 (1990).
[55] S. N. Khanna and S. Linderoth, Phys. Rev. Lett. **67**, 742 (1991).
[56] T. P. Martin, Phys. Rep. **95**, 167 (1983).